Vortex ratchet effects in a superconducting asymmetric ring-shaped device

Jiangdong Ji, Jie Yuan, Ge He, Biaobing Jin, Beiyi Zhu, Xiangdong Kong, Xiaoqing Jia, Lin Kang, Kui Jin, and Peiheng Wu

Citation: Appl. Phys. Lett. **109**, 242601 (2016); doi: 10.1063/1.4971835
View online: http://dx.doi.org/10.1063/1.4971835
View Table of Contents: http://aip.scitation.org/toc/apl/109/24
Published by the American Institute of Physics

Vortex ratchet effects in a superconducting asymmetric ring-shaped device

Jiangdong Ji,[1,2] Jie Yuan,[2,a)] Ge He,[2] Biaobing Jin,[1,b)] Beiyi Zhu,[2] Xiangdong Kong,[3] Xiaoqing Jia,[1] Lin Kang,[1] Kui Jin,[2] and Peiheng Wu[1]
[1]*Research Institute of Superconductor Electronics (RISE), School of Electronic Science and Engineering, Nanjing University, Nanjing 210093, China*
[2]*National Laboratory for Superconductivity, Institute of Physics, Chinese Academy of Sciences, Beijing 100190, China*
[3]*Electron Beam Lithography Technology Research Group, Institute of Electrical Engineering, Chinese Academy of Sciences, Beijing 100190, China*

(Received 5 October 2016; accepted 15 November 2016; published online 15 December 2016)

We investigate the vortex ratchet effects in a superconducting asymmetric ring-shaped NbN device. Through transport measurements, we find that the rectified dc voltages are significantly enhanced, and we observe time-dependent asymmetric voltage waveforms over a single cycle. Our vortex ratchet device operates over a wide range of temperatures, critical currents, and magnetic fields. We demonstrate that in this asymmetric structure giant ratchet effects are mainly caused by the collective behavior of vortices, which differs clearly from one-particle vortex effects studied in conventional vortex ratchet systems. *Published by AIP Publishing.*
[http://dx.doi.org/10.1063/1.4971835]

The controlled motion of magnetic vortices in type-II superconductors has drawn intense interest for many years because it provides a natural route to understand fundamental vortex-transport properties and explore novel solid-state devices.[1,2] Recent advances in nanofabrications make it possible to investigate means of controlling flux motion in a new generation of superconducting devices, thereby producing many potential applications such as quantum computing, superconducting quantum interference devices (SQUIDs), single photon/electron detectors, and parametric amplifiers.[1,3–10] In particular, ratchet effects based on the motion of vortices have led to proposals and realizations of flux pumps and lenses, rectifiers, diodes, or switches, which enable the removal of unwanted trapped flux and the reduction of the density of vortices in samples and devices.[11–14]

In most of the previous work, ratchet systems produced by vortices based on periodic asymmetric pinning potentials and vortex matching are considered to be one-particle ratchet systems. Sequences of forward and reverse vortex ratchet behaviors had been studied in superconducting thin films with arrays of dots, antidots, or triangular magnetic dots.[15–21] In these cases, to observe clearly the vortex ratcheting, the applied field H needs to be very low and close to the matching fields, and the temperature T should be quite near the critical temperature T_c, thereby weakening background pinning. For practical applications, superconducting devices are often operated below $T_c/2$ to elicit better performance, and the applied fields must not approach the matching fields present. Recently, much attention has been also focused on the ratchet behavior in superconducting wires with asymmetric edges or sharp turns, the geometry of which is commonly used in a variety of superconducting bridges or circuits.[8,22–25] Nevertheless, in such structures, some details are far from being completely understood and the values of some parameters need optimizing.

In this work, we investigate the vortex ratchet effects in a microscopic superconducting asymmetric ring-shaped device. This unique type of structure highlights more the collective motion of vortices. Such a structure is simple and easy to fabricate lithographically. It primarily reflects the influence of the ring-shaped geometry on vortex motion in various superconducting bridges and circuits (for example, because of limitations in fabrication, some sharp bends in the superconducting nanocircuits become rounded[26]). In addition, compared with conventional ratchet systems based on individual vortex effects,[15–19] our model is an open system where the multiple interaction of vortices plays a substantial role during ratcheting. The model exhibits a significant enhancement of the rectified signals and operates over a much wider range of temperatures, critical currents, and magnetic fields,[17–19] which is very attractive for practical device applications because for optimal performance, many superconducting devices are expected to work at low temperature and high current density.[5,25]

Using ultraviolet lithography and reactive ion retching, we fabricated our samples from 100-nm-thick films of NbN grown on a MgO (100) substrate. The structure of the sample consists of a widening eccentric circular loop with two current and two voltage contacts; details of the dimensions are given in the scanning electron microscopy (SEM) image in Fig. 1(a). The NbN thin film is a typical type-II superconductor with high critical temperature $T_c \sim 15.1$ K, a short superconducting coherence length $\xi(0) < 5$ nm, and a large London penetration depth $\lambda(0) > 200$ nm.[27] In addition, NbN films have excellent chemical and structural stability that create favorable conditions for applications in a variety of superconducting devices.[21,28,29] The transport measurements were performed in the standard four-probe configuration using a Physical Property Measurement System (PPMS)-Quantum Design device with temperature stability

a)Electronic mail: yuanjie@iphy.ac.cn
b)Electronic mail: bbjin@nju.edu.cn

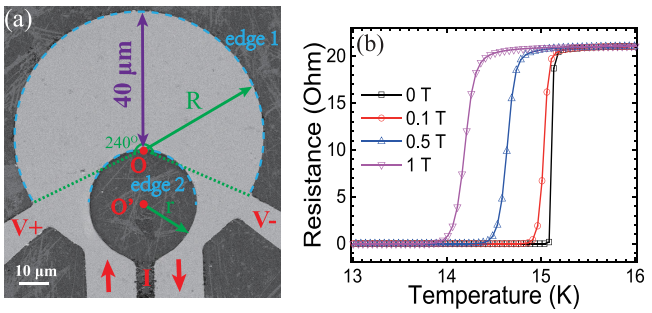

FIG. 1. (a) SEM micrograph of the sample. The geometrical parameters are $R = 40\ \mu$m, $r = 20\ \mu$m, and NbN film thickness $d = 100$ nm. (R and r are the outer and inner radii of curvature in the sample, respectively.) The widest width of the bridge is 40 μm, and the angle between the two voltage contacts is 240°. Edges 1 and 2 are the effective outer and inner edges of the bridge, respectively. The length of edge 1 is $L_1 = 167.6\ \mu$m and that of edge 2 is $L_2 = 62.8\ \mu$m. (b) Resistance vs temperature dependence of the studied sample for magnetic fields $H = 0$, 0.1, 0.5, and 1 T.

better than 0.5 mK. Figure 1(b) shows $R(T,H) - T$ plots for our sample measured in different applied magnetic fields. The field dependence of the critical temperature T_c and the sharp resistive superconducting (SC) transition with a width ΔT_c confirm the good quality of our NbN films.

To analyze the ratchet effect, a sinusoidal current $I(t) = I_{ac}\sin(2\pi ft)$, where I_{ac} is the amplitude and f is the frequency (from 0.1 kHz to 100 kHz), was generated using a current source (Model 6221, Keithley); a digital nanovoltmeter (Model 2182a, Keithley) was used to measure the average ratchet dc response, and the time-resolved voltage was recorded using an oscilloscope with a preamplifier (MDO4000, Tektronix). During the measurement, the applied magnetic field **H** stayed perpendicular to the film plane. To improve the efficacy and accuracy of measurements, all instruments were interfaced and controlled by computer operating within the LabVIEW software environment, which facilitated the capture and storage of experimental data.

The origin of the ratchet mechanism is illustrated using the model in Fig. 2. In this bridge, the Lorentz force $\mathbf{F}_L$ generated by the applied current moves the vortices along the direction of equipotential lines, which are vertical to the outer edge (edge 1) and inner edge (edge 2) of the bridge. If

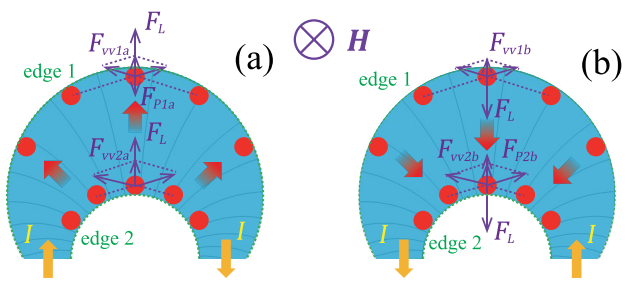

FIG. 2. Sketch of vortex motions in the bridge for opposite current directions. **H** and **I** are the applied magnetic field and the driving current, respectively. $\mathbf{F}_L$ is the Lorentz force induced by the applied current, $\mathbf{F}_p$ the pinning force determined by the edge of the bridge, and $\mathbf{F}_{vv}$ the repulsive vortex–vortex interaction force. Red circles indicate vortices (shown schematically not in scale) and red arrows show the direction in which these vortices flow. Edges 1 and 2 correspond to the outer and inner edges of the bridge; the curve lines in the sample that are vertical to both edges 1 and 2 are equipotential lines.

the current is injected along the bridge [see Fig. 2(a)], the vortices move from the inner to the outer edge. While the current is reversed, the directions of vortices also reverse [Fig. 2(b)]. When entering the bridge, the vortices feel the vortex–vortex interaction forces $\mathbf{F}_{vv2a}$ ($\mathbf{F}_{vv1b}$) near edge 2 (edge 1); when exiting the bridge, the vortices feel the vortex–vortex interaction forces $\mathbf{F}_{vv1a}$ ($\mathbf{F}_{vv2b}$) and the edge pinning force $\mathbf{F}_{p1a}$ ($\mathbf{F}_{p2b}$) near edge 1 (edge 2). We find that the vortex density is higher and the distances between vortices are shorter near edge 2 than near edge 1. In addition, this structural asymmetry of the device makes it easier (harder) for vortices to enter and exit the bridge if current flows along the bridge, as seen in Fig. 2(a) (Fig. 2(b)).

As a result, the structure of the inner and outer edges of the bridge provides significant effective potentials during vortex ratcheting. The forces acting on the vortices and the vortex motions depend on the applied current directions. We have demonstrated that such a simple unique bridge structure does contribute to the asymmetry of the $V(I)$ characteristics and therefore to vortex ratchet effects.

Figure 3 shows the dc voltage versus ac-current amplitude $(V_{dc} - I_{ac})$ characteristics at $H = 0.1$ T and $T = 14$ K. The rectification of the vortex motion is characterized by measurements of V_{dc}, which grow monotonically with I_{ac} from zero up to a maximum value of ~1.7 mV and thereafter decays smoothly to zero, thus establishing the typical behavior of ac-driven objects in a ratchet potential. The range of amplitude ΔI_{ac} where ratcheting occurs is about 7 mA, which we refer to as the rectification window. In Fig. 3 (insets I–VIII), we show details of the $(V_{dc} - I_{ac})$ characteristics by investigating the voltage output wave form over a single cycle of the ac drive for different drive amplitudes.

From insets II to III, the ratchet system acts as a half-wave rectifier, where the positive voltage wave-forms become gradually higher; in addition, V_{dc} increases. These points correspond to instances when vortices travel across the bridge only in the easy direction. At about $I_{ac} = 11$ mA (inset IV), a maximum V_{dc} is achieved and a small negative voltage sign appears in the $V(t)$ wave form, where a few

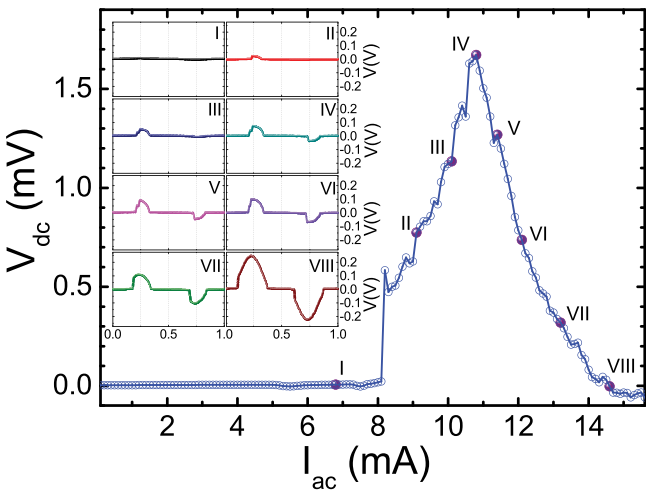

FIG. 3. DC voltage V_{dc} as a function of ac amplitude at $T = 14$ K, $H = 0.1$ T, and a frequency of $f = 1$ kHz. Insets (I–VIII): Time evolution of the voltage output $V(t)$ for one period at $I_{ac} = 7$, 9, 10, 10.8, 11.5, 12, 13.2, and 14.6 mA, respectively.

vortices are traveling in the hard direction. With a further increase in I_{ac}, both positive and negative voltage outputs gradually increase and broaden while the spacing between them decreases (insets V–VII), corresponding to the range in amplitude where V_{dc} decays.

To further illustrate the dependence of ratchet features on vortex size and density, we show in Fig. 4 the $(V_{dc} - I_{ac})$ characteristics at different temperatures for magnetic fields $H = 0.1$ T and $H = 1$ T. When $H = 0.1$ T, with increasing temperature towards T_c, our sample exhibits monotonic declines in both the maximum rectified voltage (from ~3.2 mV to ~0.5 mV) and the width of the rectification window (from ~9 mA to ~5 mA) [Fig. 4(a)]. As also seen in Fig. 4(b), with decreasing temperature, the maximum rectified dc voltage increases sharply at first, then grows more smoothly, and finally appears stable. We attribute this result to the effect of vortex fluctuations and the vortex size. When temperatures are very close to T_c, the vortex size increases significantly,

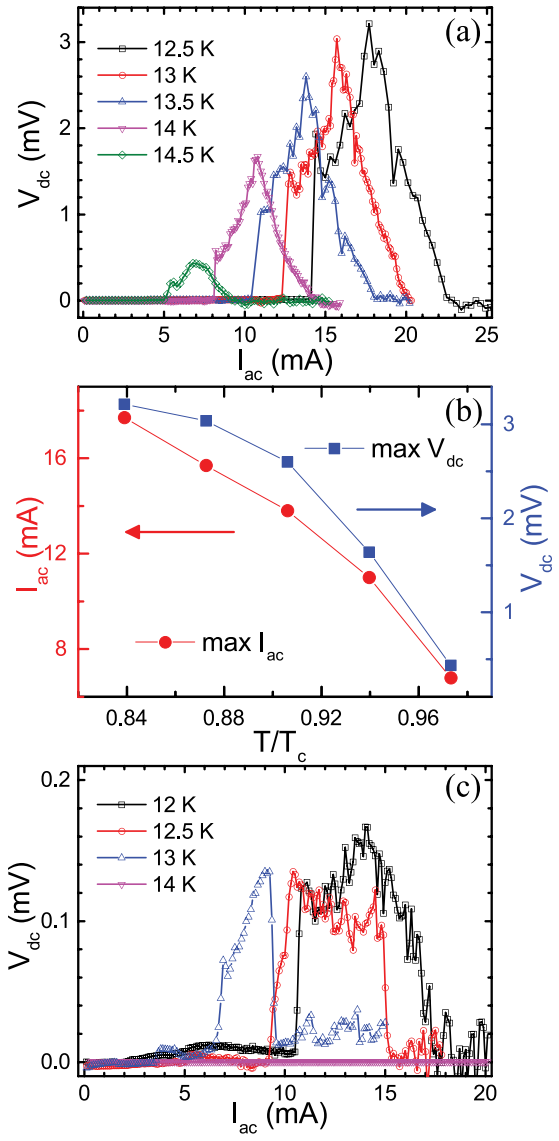

FIG. 4. (a) V_{dc} output versus ac amplitude for various temperatures $T = 12.5$, 13, 13.5, 14, and 14.5 K, with applied field $H = 0.1$ T. (b) Temperature dependent plot of the maximum V_{dc} and the ac current input I_{ac} where this is achieved in (a). (c) V_{dc} output versus ac amplitude for various temperatures $T = 12$, 12.5, 13, and 14 K, with applied field $H = 1$ T. The frequency is $f = 1$ kHz.

which weakens the effectiveness of the asymmetric potentials in our ratchet system and reduces the magnitude of its effect. In contrast, when the temperature is lowered from T_c, the decrease in fluctuations and vortex size should lead to a monotonic increase in rectification. Nevertheless, with further decreasing temperature, the vortex–vortex repulsion $\mathbf{F}_{vv}$ weakens, while both the edge pinning potential $\mathbf{F}_p$ and background pinning strengthen, thereby causing a reduction in the ratchet potential and a saturation of the rectification efficiency. In addition, the ac current amplitude where the maximum V_{dc} is achieved (the max I_{ac} in Fig. 4(b)) shifts towards higher values when the temperature decreases; this is approximately proportional to the critical current for the range of temperatures used. The variation of V_{dc} with temperature in our ratchet system is very similar to that seen in previous vortex ratchet behavior. However, this system is still able to display strong ratchet features even at low temperatures ($T/T_c = 12.5\,\text{K}/14.9\,\text{K} \approx 0.84$), which is the main difference compared with that in other work.[15–19]

As seen in Fig. 4(c), the vortex ratchet effect is much weaker at a higher magnetic field ($H = 1$ T), but the maximum dc voltage is still above 0.1 mV. At $T = 14$ K, where the temperature is very close to T_c, no ratchet signal is observed; at lower temperatures, the maximum dc voltage increases, which is similar to the behavior at $H = 0.1$ T. The reduction in the rectified voltage is explained as an increase in vortex density. In this case, the vortices cannot sense the asymmetric ratchet potential imposed by the edges of the sample. Consequently, the vortex rectification here strongly depends on the magnetic fields, but the fields will not be limited by the matching field.

Note that our system shows a significant enhancement in dc voltage rectified responses (several mV) and can operate over wide ranges of ac current amplitudes ($\Delta I_{ac} \approx 9$ mA), temperature ($T/T_c \approx 0.84$), and magnetic field ($H = 1$ T).

The rectified voltage response remains almost unchanged as frequencies are varied (from 0.1 kHz to 100 kHz) for both $H = 0.1$ T and $H = 1$ T; this demonstrates that the dc voltage is insensitive to low frequencies (Fig. 5). We calculated that

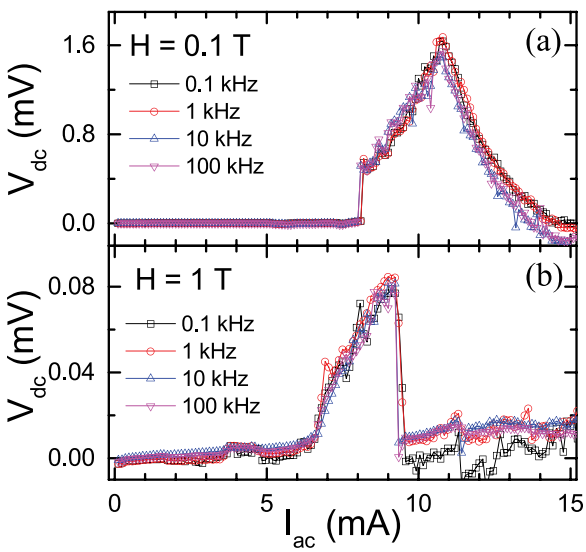

FIG. 5. V_{dc} as a function of ac amplitude I_{ac} for (a) $H = 0.1$ T and (b) $H = 1$ T at different ac frequencies. The temperature is $T = 13$ K.

the vortex velocity is $v = 100\,\mathrm{m/s}$ if the vortex does not travel across the sample during a positive half-period $T/2$. The net vortex displacement is $s = v \cdot t = vT/2 \leq w = 40\,\mu\mathrm{m}$, so $T \leq 8 \times 10^{-7} < 10^{-6}$, and therefore we have $f > 10^6\,\mathrm{Hz} = 1\,\mathrm{MHz}$. Accordingly, to achieve the distinctive step structure in the voltage versus the ac current amplitude and investigate the approximate nonadiabatic ratcheting characteristics, the applied frequency should be larger than several MHz.[30]

In summary, we have studied vortex ratchet behaviors in a unique asymmetric superconducting structure. We found that the vortex ratchet is mainly generated by a collective behavior of the vortices, from which it can be seen that both the vortex–vortex interaction and the geometry of the pinning centers play an important role in controlling the rectification of the vortex motion. Different from conventional vortex ratchet effects, our vortex ratchet system can significantly increase the ratchet signal and operate within wide ranges of temperatures, magnetic fields, and ac drive amplitudes. Moreover, our model is distinguished by its simple geometry and easy fabrication; the structure furthermore is typical and common in superconducting devices, thereby having the potential for many compatible applications.

Finally, it should be noted that this study has concentrated on only a single sample with a constant shape, thickness, and width. For similar geometries, it will be interesting to study the corresponding vortex motion when the shape of the sample is tuned or the size of sample is on the scale of the coherence length ξ or penetration length λ. Nevertheless, our results clearly indicate the main ratchet features prompting the need for further exploration of the flux motion in these micro-nanostructured superconductors.

This work was supported by the MOST973 (Grant No. 2014CB339800), the National Instrumentation Program (Grant No. 2012YQ14005), the National Natural Science Foundation (Grant Nos. 61371035, 11173015, 11227904, 61521001, and 61501219), the Priority Academic Program Development of Jiangsu Higher Education Institutions, and the Jiangsu Provincial Key Laboratory of the Advanced Manipulation of Electromagnetic Wave. B. B. Jin also acknowledges support from the Cooperative Innovation Centre of Terahertz Science, University of Electronic Science and Technology, Chengdu, China.

[1]P. Hänggi and F. Marchesoni, Rev. Mod. Phys. **81**, 387 (2009).
[2]B. L. T. Plourde, IEEE Trans. Appl. Supercond. **19**, 3698 (2009).
[3]A. Wallraff, D. I. Schuster, A. Blais, L. Frunzio, R.-S. Huang, J. Majer, S. Kumar, S. M. Girvin, and R. J. Schoelkopf, Nature **431**, 162 (2004).
[4]S. Ooi, S. Savel'ev, M. B. Gaifullin, T. Mochiku, K. Hirata, and F. Nori, Phys. Rev. Lett. **99**, 207003 (2007).
[5]N. Marrocco, G. P. Pepe, A. Capretti, L. Parlato, V. Pagliarulo, G. Peluso, A. Barone, R. Cristiano, M. Ejrnaes, A. Casaburi, N. Kashiwazaki, T. Taino, H. Myoren, and R. Sobolewski, Appl. Phys. Lett. **97**, 092504 (2010).
[6]A. Kremen, S. Wissberg, N. Haham, E. Persky, Y. Frenkel, and B. Kalisky, Nano Lett. **16**, 1626 (2016).
[7]A. Semenov, I. Charaev, R. Lusche, K. Ilin, M. Siegel, H.-W. Hübers, N. Bralović, K. Dopf, and D. Yu. Vodolazov, Phys. Rev. B **92**, 174518 (2015).
[8]G. R. Berdiyorov, M. V. Milosevic, and F. M. Peeters, Appl. Phys. Lett. **100**, 262603 (2012).
[9]M. Rosticher, F. R. Ladan, J. P. Maneval, S. N. Dorenbos, T. Zijlstra, T. M. Klapwijk, V. Zwiller, A. Lupascu, and G. Nogues, Appl. Phys. Lett. **97**, 183106 (2010).
[10]B. H. Eom, P. K. Day, H. G. LeDuc, and J. Zmuidzinas, Nat. Phys. **8**, 623 (2012).
[11]C. S. Lee, B. Jankó, I. Derényi, and A. L. Barabási, Nature **400**, 337 (1999).
[12]J. F. Wambaugh, C. Reichhardt, C. J. Olson, F. Marchesoni, and F. Nori, Phys. Rev. Lett. **83**, 5106 (1999).
[13]B. Y. Zhu, F. Marchesoni, and F. Nori, Phys. Rev. Lett. **92**, 180602 (2004).
[14]C. J. Olson, C. Reichhardt, B. Janko, and F. Nori, Phys. Rev. Lett. **87**, 177002 (2001).
[15]C. C. de Souza Silva, J. Van de Vondel, B. Y. Zhu, M. Morelle, and V. V. Moshchalkov, Phys. Rev. B **73**, 014507 (2006).
[16]B. Y. Zhu, F. Marchesoni, V. V. Moshchalkov, and F. Nori, Phys. Rev. B **68**, 014514 (2003).
[17]J. E. Villegas, S. Savel'ev, F. Nori, E. M. Gonzalez, J. V. Anguita, R. Garćia, and J. L. Vicent, Science **302**, 1188 (2003).
[18]J. Van de Vondel, C. C. de Souza Silva, B. Y. Zhu, M. Morelle, and V. V. Moshchalkov, Phys. Rev. Lett. **94**, 057003 (2005).
[19]C. C. de Souza Silva, J. Van de Vondel, M. Morelle, and V. V. Moshchalkov, Nature **440**, 651 (2006).
[20]C. Reichhardt, D. Ray, and C. J. Olson Reichhardt, Phys. Rev. B **91**, 184502 (2015).
[21]A. D. Thakur, S. Ooi, S. P. Chockalingam, J. Jesudasan, P. Raychaudhuri, and K. Hirata, Appl. Phys. Lett. **94**, 262501 (2009).
[22]O.-A. Adami, D. Cerbu, D. Cabosart, M. Motta, J. Cuppens, W. A. Ortiz, V. V. Moshchalkov, B. Hackens, R. Delamare, J. Van de Vondel, and A. V. Silhanek, Appl. Phys. Lett. **102**, 052603 (2013).
[23]D. Y. Vodolazov and F. M. Peeters, Phys. Rev. B **72**, 172508 (2005).
[24]M. Morelle, N. Schildermans, and V. V. Moshchalkov, Appl. Phys. Lett. **89**, 112512 (2006).
[25]H. L. Hortensius, E. F. C. Driessen, T. M. Klapwijk, K. K. Berggren, and J. R. Clem, Appl. Phys. Lett. **100**, 182602 (2012).
[26]M. K. Akhlaghi, H. Atikian, A. Eftekharian, M. Loncar, and A. Hamed Majedi, Opt. Express **20**, 23610 (2012).
[27]L. Kang, B. B. Jin, X. Y. Liu, X. Q. Jia, J. Chen, Z. M. Ji, W. W. Xu, P. H. Wu, S. B. Mi, A. Pimenov, Y. J. Wu, and B. G. Wang, J. Appl. Phys. **109**, 033908 (2011).
[28]G. Grimaldi, A. Leo, A. Nigro, A. V. Silhanek, N. Verellen, V. V. Moshchalkov, M. V. Milosevic, A. Casaburi, R. Cristiano, and S. Pace, Appl. Phys. Lett. **100**, 202601 (2012).
[29]S. P. Chockalingam, M. Chand, J. Jesudasan, V. Tripathi, and P. Raychaudhuri, Phys. Rev. B **77**, 214503 (2008).
[30]B. B. Jin, B. Y. Zhu, R. Wördenweber, C. C. de Souza Silva, P. H. Wu, and V. V. Moshchalkov, Phys. Rev. B **81**, 174505 (2010).